

HIGH-REDSHIFT STAR FORMATION EFFICIENCY AS UNCOVERED BY THE IRAM PHIBSS PROGRAMS

J. Freundlich¹, P. Salom ¹, F. Combes¹, L. Tacconi², R. Neri³, S. Garcia-Burillo⁴, R. Genzel^{2,5,6}, T. Contini^{7,8}, S. Lilly⁹ and the PHIBSS Consortium

Abstract. The evolution of the cosmic star formation rate (SFR) is characterized by a peak around redshift $z=2-3$ and a subsequent drop by an order of magnitude. High levels of star formation are sustained by a continuous supply of fresh gas and high molecular gas fractions. But once galaxies exceed a certain mass or enter a harsh environment, star formation is quenched, and different phenomena could explain the resulting evolution of the cosmic SFR. Is it mostly driven by the available molecular gas, or because star formation processes are more efficient at high redshift? Here we present the results and the perspectives of the PHIBSS programs, which aim at understanding early galaxy evolution and the winding-down of star formation from the perspective of the galaxies' molecular gas reservoirs. These programs use statistically meaningful samples of galaxies belonging to the massive end of the star formation main-sequence at different redshifts. The previous IRAM PHIBSS program has already uncovered large molecular gas reservoirs at redshifts $z\sim 1-2$, with gas fractions 4 to 10 times higher than in the local Universe, and the ongoing IRAM and ALMA programs extend the sample to a wider range of redshifts and to a more complete sampling of the stellar mass-SFR plane. The IRAM PHIBSS2 legacy program is designed to make full use of the upcoming NOEMA capabilities.

Keywords: galaxies: evolution, galaxies: high-redshift, galaxies: structure, stars: formation, galaxies: ISM

1 Introduction

Our Galaxy only forms a few stars per year, as most nearby spiral galaxies. But ten billion years ago, between redshifts 2 and 3, observed galaxies formed their stars at rates up to 20 times higher (Noeske et al. 2007; Daddi et al. 2007). What are the causes of the decrease of the star formation activity after this peak?

Stars are formed from cold molecular gas clouds which collapse due to their gravitational pull. A high star formation rate (SFR) thus means a significant gas content, either brought by major mergers or by continuous processes such as smoother gas accretion along streams of the cosmic web (Kere  et al. 2005; Dekel et al. 2009a). Observations show that high-redshift galaxies near the star formation peak are indeed much more gas-rich and clumpy than their low-redshift counterparts (Daddi et al. 2010; Tacconi et al. 2010; F rster Schreiber et al. 2011), but many other parameters may intervene, from environmental effects, morphological quenching, and feedback mechanisms from stars and AGN, to the star formation efficiency itself ($SFE=SFR/M_{\text{gas}}$). This latter quantity has notably been shown to decrease significantly after $z = 1$ (Combes et al. 2011, 2013) and could thus contribute substantially to the evolution of the cosmic SFR. Is the evolution of the cosmic SFR after

¹ LERMA, Observatoire de Paris, CNRS, 61 av. de l'Observatoire, 75014 Paris, France

² Max-Planck-Institut f r Extraterrestrische Physik (MPE), Giessenbachstrasse 1, 85748 Garching, Germany

³ IRAM, 33 rue de la Piscine, 38406 St. Martin d'H res, Grenoble, France

⁴ Observatorio Astron mico Nacional (OAN), Apartado 1143, 28800 Alcal  de Henares, Madrid, Spain

⁵ Dept. of Physics, Le Conte Hall, University of California, CA 94721 Berkeley, USA

⁶ Dept. of Astronomy, Campbell Hall, University of California, CA 94721 Berkeley, USA

⁷ Institut de Recherche en Astrophysique et Plan tologie (IRAP), CNRS, 14 av.  douard Belin, 31400 Toulouse, France

⁸ IRAP, Universit  de Toulouse, UPS-OMP, Toulouse, France

⁹ Institute for Astronomy, Department of Physics, ETH Zurich, CH-8093 Zurich, Switzerland

the star formation peak mostly driven by the declining cold gas reservoir, or are the star formation processes qualitatively different at the corresponding redshifts?

If the averaged evolution of the cosmic SFR displays a peak around $z=2-3$ and a subsequent drop by an order of magnitude, the galaxy distribution is far from homogeneous. There is indeed a bimodality between blue star-forming disks on one side and red passive galaxies on the other. The blue star-forming galaxies lie on a tight relationship in the stellar mass-SFR plane, the main sequence of star formation (MS; Noeske et al. 2007; Elbaz et al. 2007; Daddi et al. 2007; Wuyts et al. 2011). At a given stellar mass M_* , the SFR on the MS drops by a factor ~ 20 from $z \sim 2$ to the present time. Typical star-forming galaxies are expected to follow the MS until their star formation activity is quenched, and then to rapidly transit down to the red sequence (e.g., Bouché et al. 2010). This transition is still poorly understood.

The PHIBSS programs study the molecular gas properties of star-forming galaxies on and around the MS and aim at better understanding the winding-down of star formation and the quenching processes with a statistical sample of galaxies at high redshift. Cold molecular gas is traced through the CO rotational lines, and the programs also include high-resolution observations to study the star formation efficiency at sub-galactic scales. The main goals of the PHIBSS programs are to study the evolution with redshift of the molecular gas fraction (f_{gas}) and the SFE in normal MS star-forming galaxies, to characterize the dependence of these quantities on stellar mass and morphology in order to compare with feedback and quenching models, to examine the inner gas dynamics, and to probe the physical gas properties through multiple CO transitions. The first IRAM PHIBSS Large Program (L. Tacconi, F. Combes, et al.) focussed on the massive tail ($M_* > 3.10^{10} M_\odot$) of the MS at $z=1.2$ and 2.2 and comprised 52 CO detections and 8 high-resolution imaging observations, while the ongoing PHIBSS2 programs triple the number of observed galaxies and better sample the M_* -SFR plane. Here we focus on the results of the first IRAM PHIBSS program concerning the star formation efficiency, first from the galaxy-averaged observations, and then from the resolved observations.

2 Galaxy-averaged star formation relations

The IRAM PHIBSS Large Program first enables to characterize the galaxy-averaged properties of the molecular gas in high-redshift MS galaxies, and to study their evolution with redshift. It notably shows that most of these galaxies are clumpy disks, as the two galaxies displayed in the left panel of Fig. 1 (Tacconi et al. 2010, 2013). The PHIBSS program also confirms the presence of large molecular gas fractions in high-redshift MS galaxies, with mean values reaching 33% at $z \sim 1.2$ and 47% at $z \sim 2.2$ (Tacconi et al. 2013). This is to be compared with the 8% that are observed at $z=0$ (Leroy et al. 2008; Saintonge et al. 2011). Gas-rich disks are more likely to be gravitationally unstable, and thus to display clumpy features and to form stars.

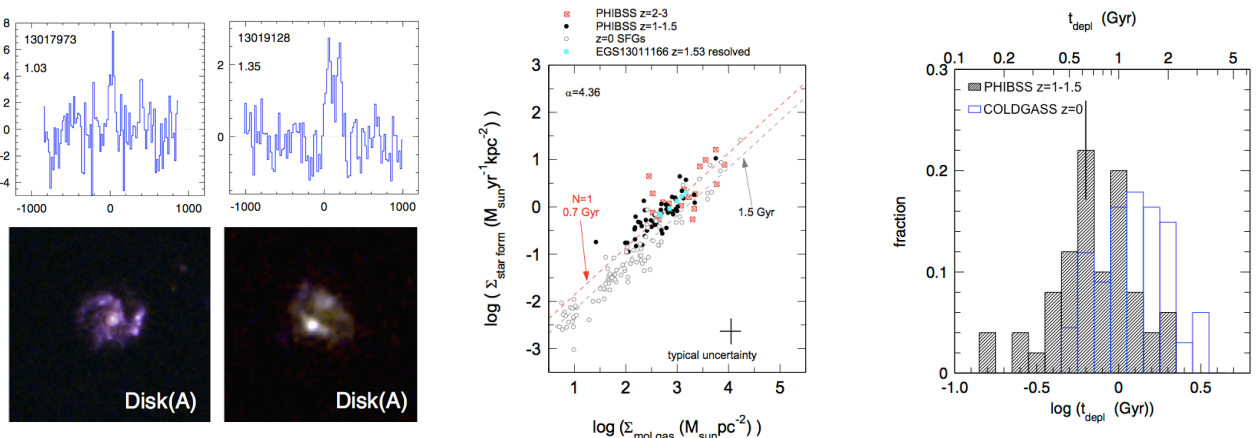


Fig. 1. HST images and galaxy-integrated CO velocity spectra for two galaxies from the PHIBSS program, displaying disk-like features (left); the near-linear KS scaling relation between the molecular gas and SFR surface densities (middle); and the distribution of depletion times (right). In the last two plots, the PHIBSS high-redshift data points are compared to $z=0$ samples. Whereas the galaxy-averaged KS relation is comparable at low and high redshifts, the slight decrease of the depletion time with redshift might indicate a more efficient star formation at high redshift (Tacconi et al. 2013).

The Kennicutt-Schmidt (KS) relation between the gas and SFR densities characterizes the star formation efficiency, and is shown to be near linear at low redshift (Kennicutt 1998; Kennicutt & Evans 2012). As shown in the middle panel of Fig. 1, the same trend is observed at $z=1-3$ for the galaxies of the PHIBSS sample (Genzel et al. 2010; Tacconi et al. 2013). Nevertheless, the mean depletion time ($t_{\text{depl}} = M_{\text{gas}}/\text{SFR}$) of 0.7 Gyr is slightly lower than at present time: as this timescale represents the time needed for a galaxy to consume all its gas in order to form stars, it implies a faster star formation duty cycle and a need for gas replenishment at the peak of the star formation activity. The right panel of Fig. 1 compares the distribution of depletion times in the PHIBSS high-redshift sample with the COLDGASS sample at $z=0$. The depletion time is the inverse of the SFE, which could thus be slightly higher at high-redshift.

The PHIBSS program also shows that the specific star formation rate ($\text{sSFR} = \text{SFR}/M_{\text{star}}$) correlates strongly with the gas fraction: the variation of the sSFR between $z=3$ and $z=0$, as well as the vertical offset of a galaxy from the MS in the M_{\star} -SFR plane, are mainly controlled by the molecular gas fraction (Tacconi et al. 2013).

3 Resolved kinematics and star formation relations at sub-galactic scales

The IRAM PHIBSS program also includes high-resolution observations of the molecular gas for a subsample of 8 galaxies, carried at the IRAM Plateau de Bure interferometer. The angular resolution attained by these observations reaches $0.3''-1''$, which enables to fathom star formation processes at sub-galactic scales, as $1''$ notably corresponds to ~ 8 kpc at $z=1.2$.

Sub-arcsecond galaxy kinematics give access to good quality rotation curves and to the velocity dispersion. The left panel of Fig. 2 shows the superposition of two HST broad-band images with the CO high-resolution observations for one galaxy from the PHIBSS sample, as well as its velocity and velocity dispersion maps, and its rotation curve (Tacconi et al. 2010). A rotating disk is clearly visible. The high-redshift disks are more turbulent by a factor ~ 5 than their low-redshift counterparts (Tacconi et al. 2013), which is compatible with models where clumpy cosmic streams feed the disk and trigger violent gravitational instabilities (e.g., Dekel et al. 2009b).

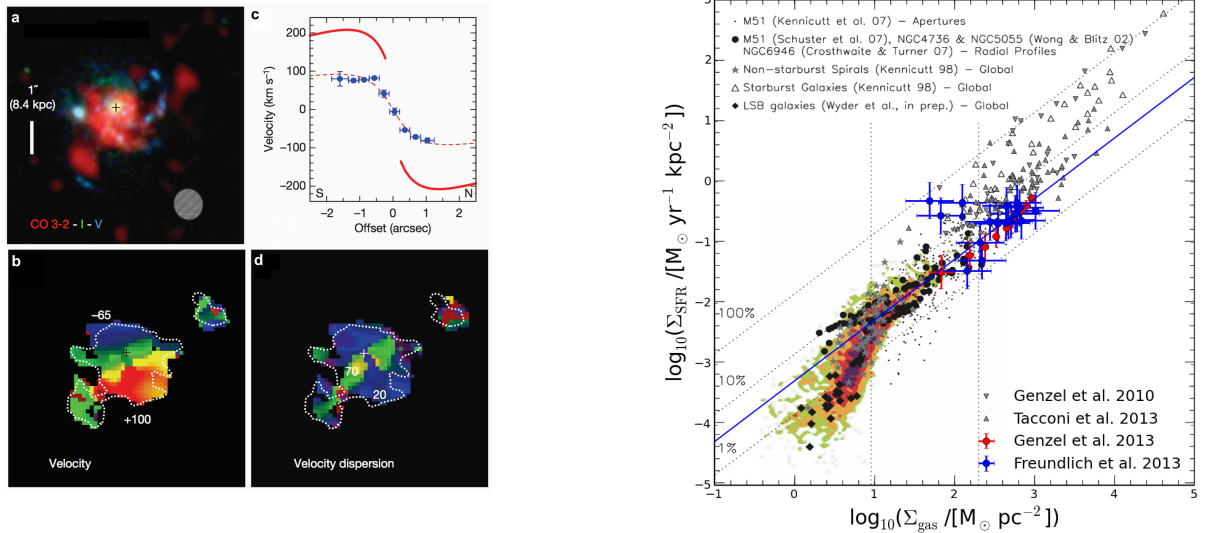


Fig. 2. Left: (a) CO line emission with HST I and V bands images of the $z=1.2$ source EGS13035123; (b) its velocity map; (c) the corresponding rotation curve, with the best fitting exponential disk model indicated as a dashed line; and (d) the velocity dispersion map deduced by subtracting the modeled rotation to the observed velocity (Tacconi et al. 2010). Right: Spatially resolved molecular KS relation for ensembles of clumps of four galaxies from the PHIBSS sample (Freundlich et al. 2013) and for binned groups of pixels in EGS13011166 (Genzel et al. 2013), superimposed on the sub-galactic KS diagram obtained at low redshift by Bigiel et al. (2008). The solid blue line corresponds to a constant depletion time $t_{\text{depl}} = 1.9$ Gyr, and the grey data points to galaxy-averaged measurements.

Resolved kinematics also enables to separate smoothed ensembles of clumps due to their different velocities, and to obtain a resolved KS relation averaged at a scale of about $1''$ (8 kpc) for four galaxies of the PHIBSS sample (Freundlich et al. 2013). The CO line luminosity from the IRAM observations traces the cold molecular gas, while the [OII] line from Keck DEEP2 spectra is empirically calibrated to trace the SFR. The results are compatible with a linear relation and a constant depletion time of 1.9 Gyr, and fit well with the corresponding low-redshift observations, as shown in the right panel of Fig. 2. These results seem to point towards similar star formation processes at high and low redshifts, but a bigger statistical sample would be necessary to obtain more meaningful mean depletion times for the substructures of high-redshift galaxies.

Genzel et al. (2013) further obtain a pixel by pixel KS relation for one typical $z=1.53$ massive star-forming galaxy from the PHIBSS sample, EGS13011166, and take into account extinction and $H\alpha$ observations to show that the shape and the slope of the KS relation depend strongly on the extinction correction that is applied. Using resolved extinction maps instead of a single value for the whole galaxy significantly changes the depletion times that are obtained from sub-galactic observations.

4 Conclusion and perspectives

The IRAM PHIBSS survey shows that the evolution of the cosmic SFR is mostly driven by the available gas reservoir, but the slightly shorter depletion times that are observed might also indicate that star formation is somewhat more efficient at high redshift. On sub-galactic scales, it was possible to draw a KS relation for ensembles of clumps of four massive galaxies at $z=1.2$ and on a pixel basis for one galaxy at $z=1.53$.

The ongoing IRAM PHIBSS2 Legacy Program (F. Combes, S. Garcia-Burillo, R. Neri, L. Tacconi, et al.) will more than triple the number of high-redshift normal star-forming galaxies with CO measurements, extend their redshift range, and include galaxies below the MS. This four year program is phased to optimize and exploit the NOEMA capabilities as they come online: the smaller integration times and the increased sensitivity will permit a statistical gain and a better sampling of the M_{\star} -SFR plane. Complementary ALMA programs will further contribute to extend the sample owing to an even higher sensitivity (R. Genzel et al.), probe higher CO transitions to study the gas excitation and the physical conditions of the gas in early star-forming systems (A. Weiss et al.), and possibly obtain high-resolution images and kinematics of the molecular gas in galaxies at intermediate redshifts (Freundlich et al.).

References

- Bigiel, F., Leroy, A., Walter, F., et al. 2008, *AJ*, 136, 2846
 Bouché, N., Dekel, A., Genzel, R., et al. 2010, *ApJ*, 718, 1001
 Combes, F., García-Burillo, S., Braine, J., et al. 2011, *A&A*, 528, A124
 Combes, F., García-Burillo, S., Braine, J., et al. 2013, *A&A*, 550, A41
 Daddi, E., Bournaud, F., Walter, F., et al. 2010, *ApJ*, 713, 686
 Daddi, E., Dickinson, M., Morrison, G., et al. 2007, *ApJ*, 670, 156
 Dekel, A., Birnboim, Y., Engel, G., et al. 2009a, *Nature*, 457, 451
 Dekel, A., Sari, R., & Ceverino, D. 2009b, *ApJ*, 703, 785
 Elbaz, D., Daddi, E., Le Borgne, D., et al. 2007, *A&A*, 468, 33
 Förster Schreiber, N. M., Shapley, A. E., Genzel, R., et al. 2011, *ApJ*, 739, 45
 Freundlich, J., Combes, F., Tacconi, L. J., et al. 2013, *A&A*, 553, A130
 Genzel, R., Tacconi, L. J., Gracia-Carpio, J., et al. 2010, *MNRAS*, 407, 2091
 Genzel, R., Tacconi, L. J., Kurk, J., et al. 2013, *ApJ*, 773, 68
 Kennicutt, R. C. & Evans, N. J. 2012, *ARA&A*, 50, 531
 Kennicutt, Jr., R. C. 1998, *ApJ*, 498, 541
 Kereš, D., Katz, N., Weinberg, D. H., & Davé, R. 2005, *MNRAS*, 363, 2
 Leroy, A. K., Walter, F., Brinks, E., et al. 2008, *AJ*, 136, 2782
 Noeske, K. G., Weiner, B. J., Faber, S. M., et al. 2007, *ApJ*, 660, L43
 Saintonge, A., Kauffmann, G., Kramer, C., et al. 2011, *MNRAS*, 415, 32
 Tacconi, L. J., Genzel, R., Neri, R., et al. 2010, *Nature*, 463, 781
 Tacconi, L. J., Neri, R., Genzel, R., et al. 2013, *ApJ*, 768, 74
 Wuyts, S., Förster Schreiber, N. M., van der Wel, A., et al. 2011, *ApJ*, 742, 96